UCRL-JC-125034
PREPRINT

A First Look at the New ARAC Dispersion Model

J.M. Leone, Jr.
J.S. Nasstrom
D.M. Maddix

This paper was prepared for submittal to the
American Nuclear Society's Sixth Topical Meeting
on Emergency Preparedness and Response
San Francisco, CA
April 22-25, 1997

November 1996

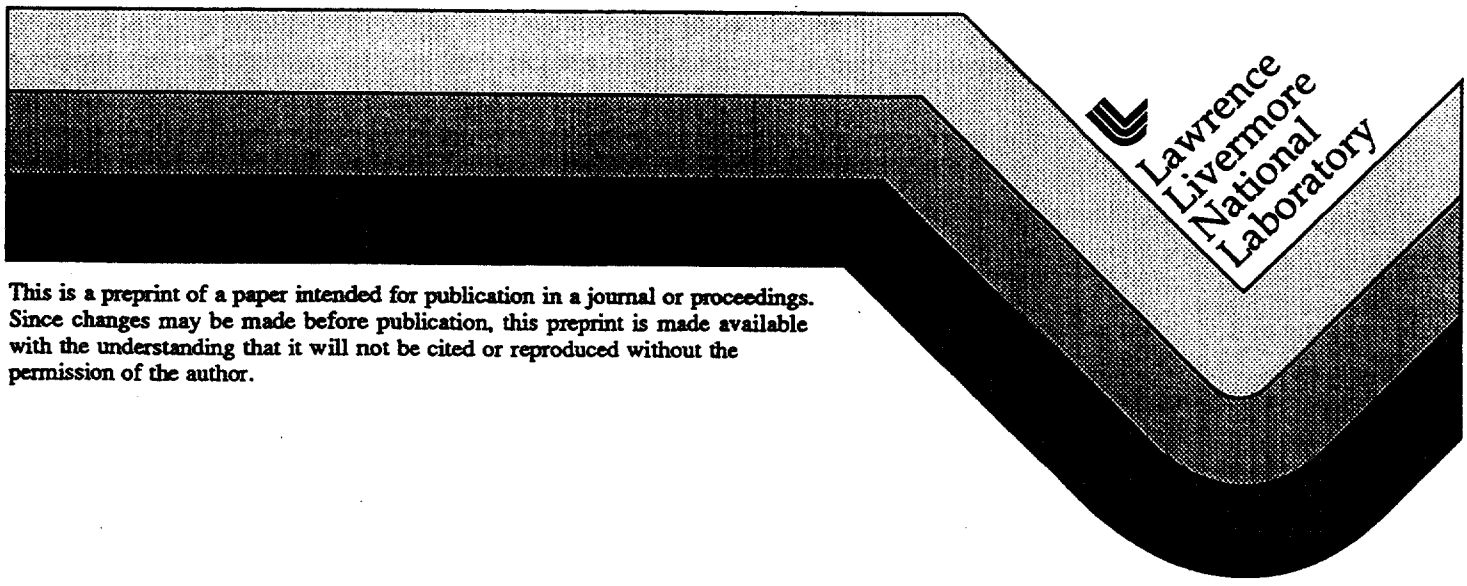

A FIRST LOOK AT THE NEW ARAC DISPERSION MODEL

John M. Leone, Jr.
Lawrence Livermore National Lab.
P.O. Box 808
Livermore, CA 94550
(510) 422-6449

John S. Nasstrom
Lawrence Livermore National Lab.
P.O. Box 808
Livermore, CA 94550
(510) 423-6738

Denise M. Maddix
Lawrence Livermore National Lab.
P.O. Box 808
Livermore, CA 94550
(510) 423-4236

SUMMARY

We describe a new atmospheric dispersion model being developed for the emergency response system of the U.S. Department of Energy's Atmospheric Release Advisory Capability (ARAC). This model solves the turbulent, advection-diffusion equation via a Lagrangian particle, Monte-Carlo method. Within a simulation, particles representing the pollutant are moved through the domain using a random displacement method to model the turbulent diffusion and a Runge-Kutta method to model the advection. The bottom boundary in the new model is a union of bilinear surfaces between gridded terrain data rather than the discontinuous "stair step" representation of terrain used previously in ARAC. The new model accepts winds on (x, y, σ_z) grids that can be horizontally and vertically graded and nested in the horizontal.

I. INTRODUCTION

The Atmospheric Advisory Capability (ARAC) at Lawrence Livermore National Laboratory provides real-time emergency response support for accidental radiological releases to the atmosphere for U.S. Department of Defense and the U.S. Department of Energy. As part of ARAC's effort to assure the best service possible to its customers, it is designing and implementing a complete new system called ARAC III. This paper presents a first look at the ARAC III atmospheric dispersion model together with some early results.

II. MODEL DESCRIPTION

ARAC has decided to continue the methodology for dispersion forecasting in ARAC III that has been so successful in the past, i.e., a separate Lagrangian particle dispersion model. This new model will solve:

$$\frac{\partial \overline{C}}{\partial t} = -\overline{u}\frac{\partial \overline{C}}{\partial x} - \overline{v}\frac{\partial \overline{C}}{\partial y} - \overline{w}\frac{\partial \overline{C}}{\partial z} + \frac{\partial}{\partial x}\left(K_x\frac{\partial \overline{C}}{\partial x}\right) + \frac{\partial}{\partial y}\left(K_y\frac{\partial \overline{C}}{\partial y}\right) + \frac{\partial}{\partial z}\left(K_z\frac{\partial \overline{C}}{\partial z}\right) \quad (1)$$

where $\overline{C}$ is the mean air concentration of the species, $\overline{u}$, $\overline{v}$, and $\overline{w}$ are the mean wind components in the x, y, and z directions respectively; t is time; and K_x, K_y, and K_z are the eddy diffusivities for the three coordinate directions.

However, rather than solve the above Eulerian equation directly, the model solves the stochastic differential equations that describe the same process within a Lagrangian framework.[1] The equations describing the particle displacement in the three coordinate directions are:

$$dx = \overline{u}dt + (2K_x)^{1/2}dW_x, \quad (2)$$

$$dy = \overline{v}dt + (2K_y)^{1/2}dW_y, \quad (3)$$

$$dz = \overline{w}dt + \frac{\partial K_z}{\partial z}dt + (2K_z)^{1/2}dW_z \quad (4)$$

where $dW_{x,y,z}$ are three independent random variates with zero mean and variance dt. (It has been assumed that turbulence is homogeneous in the horizontal, x and y, directions.)

In a simulation, the species of interest is represented by a large number of marker particles (fluid elements), each with a specified species mass. The stochastic differential equations above are integrated in time to calculate an independent trajectory of each particle. The ensemble-mean concentration at any time t can then be calculated from the particle locations at time t and the species mass associated with each particle.

The first step in any simulation is to generate the initial particle positions and characteristics. In order to do this, the

model contains a number of options to describe the source geometry: a point, a sphere with a uniform distribution of species, a line with a uniform distribution of species, and a three-dimensional Gaussian distribution. All of these source descriptions can have time varying geometric parameters and emission rates.

The integration method used to derive the particle trajectories given the particle initial positions is a two-step process. First, a random displacement method (RDM) is used to calculate the displacements due to turbulent diffusion. Thus, for a given particle at time t_i:

$$\Delta x_{i,turb} = (2K_{xi}\Delta t_i)^{1/2}\xi_{xi}, \quad (5)$$

$$\Delta y_{i,turb} = (2K_{yi}\Delta t_i)^{1/2}\xi_{yi}, \quad (6)$$

$$\Delta z_{i,turb} = \left(\frac{\partial K_z}{\partial z}\right)_i \Delta t_i + \left[2K_{zi}\Delta t_i + \left(\frac{\partial K_z}{\partial z}\right)_i^2 \Delta t_i^2\right]^{1/2} \xi_{zi}, \quad (7)$$

where, for example, $\Delta z_i = z(t_{i+1}) - z(t_i)$, $\Delta t_i = t_{i+1} - t_i$, $K_{zi} = K_z(z_i, t_i)$, $\left(\frac{\partial K_z}{\partial z}\right)_i = \left.\frac{\partial K}{\partial z}\right|_{\substack{t=t_i \\ z=z_i}}$, and ξ_{zi} is a random number with zero mean and variance one. The horizontal eddy diffusivities are based on Draxler's[2] semi-empirical relationship for σ_y and the standard deviation of the crosswind velocity component. The vertical eddy diffusivity is derived from the surface layer and boundary layer scaling parameters using the method of Lange.[3]

Next the mean wind velocities are used to calculate the final positions using a second order Runge-Kutta method.

$$\Delta x_i = \frac{1}{2}(k1_{xi} + k2_{xi}), \quad (8)$$

$$\Delta y_i = \frac{1}{2}(k1_{yi} + k2_{yi}), \quad (9)$$

$$\Delta z_i = \frac{1}{2}(k1_{zi} + k2_{zi}), \quad (10)$$

where $k1_{xi} = \bar{u}(x_i, y_i, z_i, t_i)\Delta t_i + \Delta x_{i,turb}$,

and $k2_{xi} = \bar{u}(x_i + k1_{xi}, y_i + k1_{yi}, z_i + k1_{zi}, t_i + \Delta t_i)\Delta t_i + \Delta x_{i,turb}$

and similarly for the y and z directions. The particle positions are then updated such that $x_{i+1} = x_i + \Delta x_i$, and so forth. To maintain accuracy and maximize efficiency, the model calculates a unique time step for each particle at each time. This allows using large time steps for slow-moving particles, while fast-moving particles will be tracked with a smaller time step.

While in theory the above algorithms are grid free, this is not the case in practice. First, the model must have a representation of both the domain topography to describe the bottom boundary and the mean winds. Since neither of these are generally know at every point in space, this information is in the form of gridded data.

The (x, y, σ_z) coordinate system is used for the model grids with $\sigma_z = \frac{z - z_g(x,y)}{z_{top} - z_g(x,y)}$, z_{top} the elevation of the upper boundary and $z_g(x,y)$ the surface elevation. There are two types of grids used within the model: the first are called the meteorological data grids and the second concentration grids.

The meteorological grids contain the wind components (u, v, w) at the grid points. These grids are typically graded in the vertical and may be either graded or regular in the horizontal. To accommodate output from modern mesoscale models, three meteorological grids can be nested within each other. In addition to the wind components, the terrain elevations are specified at the $\sigma_z = 0$ grid points of each meteorological grid. The bottom surface of the domain is determined by bilinear interpolation of the gridded elevations. The gridded winds are input into the model at user specified intervals. The wind at a given location and time is then calculated via tri-linear interpolation in space and linear interpolation in time.

The second grid type is the concentration grid. This grid defines the sampling cells used in the calculation of species concentration from particle positions. It is usually graded in all three directions with the smallest zones near the source.

III. APPLICATION

As an initial demonstration of the new model, we have run a simulation of the August 31, 1986 Diablo Canyon tracer experiment.[4] The Diablo Canyon tracer experiment was conducted by the Pacific Gas and Electric Company from August 31 to September 17, 1986 near San Luis Obispo on the central coast of California. This simulation is of a release of SF_6 at 71 m above ground level (AGL) from 0800 to 1000 PDT (1500-1700 UTC).

The simulation domain covers a 50 km by 50 km area in the horizontal and extends up to 3 km in the vertical. We used a

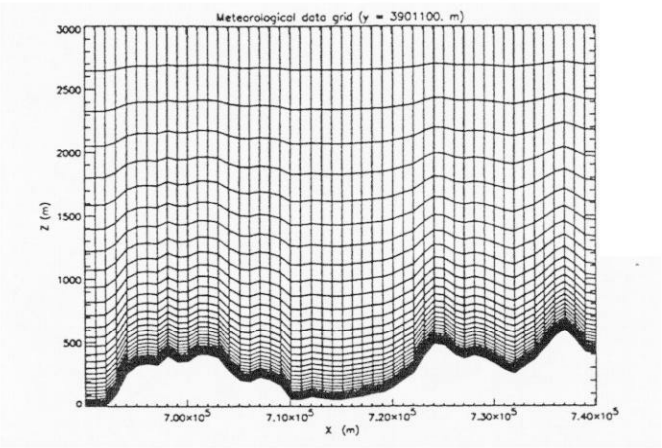

Figure 1. An x-z cross section of the meteorological grid.

single meteorological grid with a $\Delta x = \Delta y = 1$ km. Figure 1 displays a vertical (x, z) cross section of the meteorological grid displaying the graded vertical resolution. The simulation is for three hours from 0800-1100 PDT using wind data sets every 15 minutes. The wind data was processed through the ARAC III diagnostic wind modeling system.[5]

Figure 2 shows a plan view of the instantaneous position of the particles at 0900 PDT, one hour into the simulation. This figure also shows a 20 km x 20 km interior region of the concentration grid and terrain contours every 100 m. The finest horizontal resolution on the concentration grid is $\Delta x = \Delta y = 0.1$ km at the source. The low level winds during the first hour of the simulation are very light and variable and this is reflected in the bunching of the particles near the source.

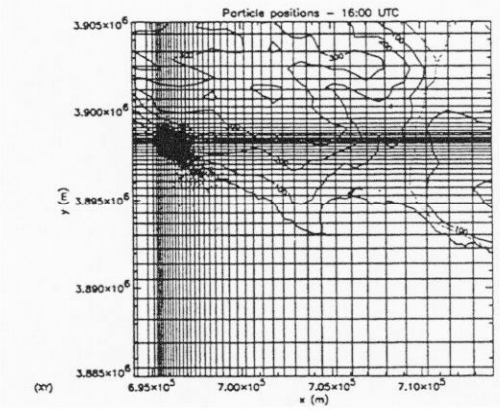

Figure 2. Plan view of the instantaneous particle postions at 0900 PDT. Also shown are the concentration grid and the terrain contours every 100 m.

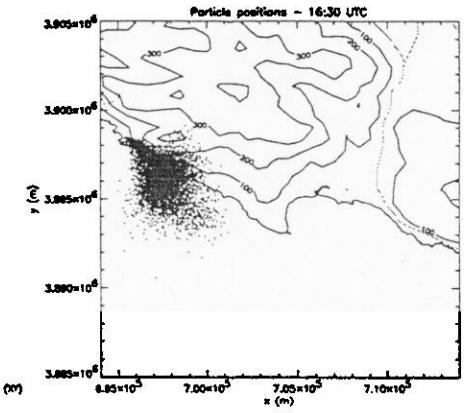

Figure 3. Plan view of the particle positions at 0930 PDT.

Figures 3 and 4 present the instantaneous particle positions (plan view) at 0930 PDT, 1.5 hours into the simulation, and 1000 PDT, two hours into the simulation, respectively. Beginning at 0900 PDT, the low level wind direction steadied, blowing southeastward along the coast with a corresponding increase in speed. This is again revealed in the particle positions in the figures. The particles moving offshore have been mixed up into the prevailing north wind above 300 m AGL.

Figure 5 shows contours of the simulated 1-hour averaged surface concentrations for 1000-1100 PDT (1700-1800 UTC) overlaid on the model terrain contours. Also, plotted are representative sampler values. (Note: all values below 50 are suspect due to fugitive emissions.) The simulated plume matches the general pattern of the measured values quite well. While the movement of the plume offshore cannot be verified, it is quite reasonable in light of the observed offshore component of the wind above 300 meters AGL.

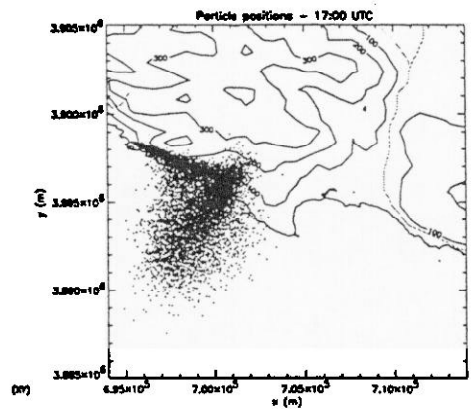

Figure 4. Plan view of the particle positions at 1000 PDT.

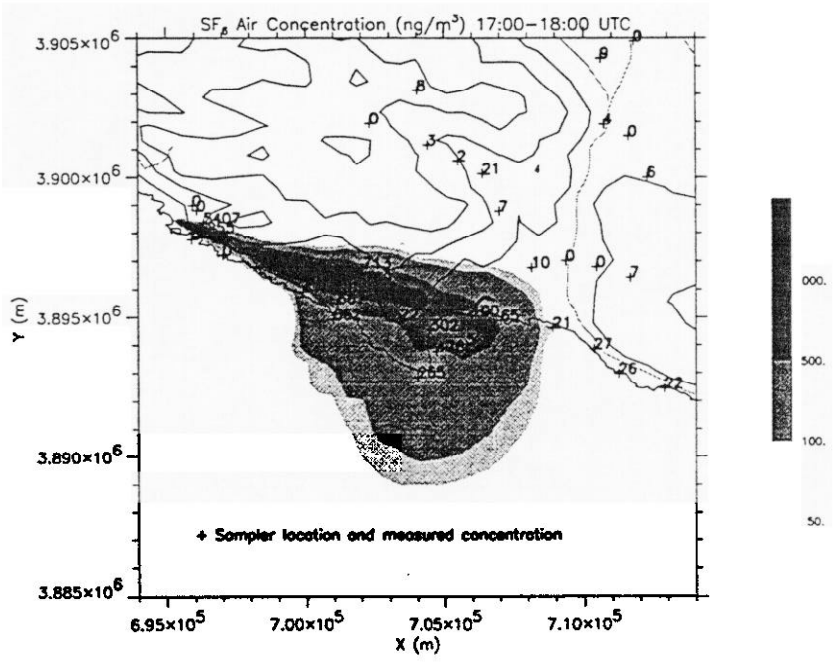

imulated
sampler values for 1000-1100 PDT.

IV. CONCLUSION

We have described an initial version of the dispersion model that will become part of ARAC's emergency response system when the ARAC III system becomes operational. Before that time, we plan to add a number of features such as buoyant and explosive plume rise, wet deposition, the ability to accept turbulent diffusivities from the mesoscale model. And, to substantiate the quality of ARAC forecasts, we will be conducting an extensive model validation program.

ACKNOWLEDGMENTS

The authors would like to thank D. Ermak for his technical guidance, H. Walker for providing the grid generation model, T. Kuczmarski for graphics support and K. Foster for aid with the experimental data. This work was performed under the auspices of the U.S. Department of Energy by the Lawrence Livermore National Laboratory under Contract No. W-7405-Eng-48.

REFERENCES:

1. B.A. Boughton, J.M. Delaurentis, and W.E. Dunn, "A Stochastic Model of Particle Dispersion in the Atmosphere," *Boundary-Layer Meteor.*, **40**, 147-163 (1987).

2. R.R. Draxler, "Determination of Atmospheric Diffusion Parameters," *Atmos. Environ.*, **10**, 99-105 (1976).

3. R. Lange, "Transferability of a Three-Dimensional Air Quality Model Between Two Different Sites in Complex Terrain," *J. Appl. Meteoro.*, **28**, 665-679 (1989).

4. R.H. Thuillier, "Tracer Experiments and Model Evaluation at Diablo Canyon Nuclear Power Plant," *Proc. of the ANS Topical Meeting on Emergency Response-Planning, Technologies, & Implementation, CONF-880913*, Amer. Nuc. Soc., LaGrange, Ill., (1988).

5. G. Sugiyama and S.T. Chan, "Meteorological Data Assimilation for Real-Time Emergency Response", *Proc. of the ANS. Sixth Topical Meeting on Emergency Preparedness and Response*, ANS., San Francisco, CA., (1997).